Direct Observation of the Ferric-Porphyrin Cation Radical as an Intermediate in the Phototriggered Oxidation of Ferric- to Ferryl-Heme Tethered to Ru(bpy)$_3$ in Reconstituted Myoglobin

Itaru Hamachi,*[,†,‡] **Shinya Tsukiji,**[†] **Seiji Shinkai,**[†] **and Shigero Oishi**[§]

Contribution from the Department of Chemistry & Biochemistry, Graduate School of Engineering, Kyushu University, Fukuoka 812-8581, Japan, Institute of Molecular Science, Myodaiji, Okazaki 444, Japan, and Department of Chemistry, School of Science, Kitasato University, Sagamihara, Kanagawa 228-8520, Japan

Received December 7, 1998

Abstract: Using semisynthetic myoglobins (Ru(bpy)$_3$-Mbs) with covalently appended Ru(bpy)$_3$ (bpy = 2,2′-bipyridine), an oxidized Mb is photoproduced through an intramolecular electron abstraction reaction as a key step. UV−vis spectra, electron paramagnetic resonance measurements, and reactivity tests identify the photooxidized Mb as a ferryl species (i.e., Fe^{4+}-heme). By circular dichroism (CD) spectroscopy, high-performance liquid chromatography (HPLC), and SDS−polyacrylamide gel electrophoresis (SDS−PAGE), it was confirmed that the photooxidation proceeds without damage of the protein structure. Significantly, we report the first direct observation of ferryl-Mb photogeneration via the intermediate porphyrin cation radical. As a consequence of this observation and proposed mechanism, the rate constants for each step can be clearly determined. The photoexcited Ru^{2+}(bpy)$_3$ is oxidatively quenched by [Co(NH$_3$)$_5$Cl]$^{2+}$, a sacrificial acceptor, to produce Ru^{3+}(bpy)$_3$, which then proceeds to abstract an electron from the porphyrin ring with a first-order rate constant of 7.1×10^5 s^{-1}, in the first step. The electron transfer is followed by iron(III) oxidation by the porphyrin radical with concurrent deprotonation (a first-order rate constant of 4.0×10^4 s^{-1} at pH 7.5, and 2.0×10^5 s^{-1} at pH 9.0) in the second step. Consistent with this mechanism, it is demonstrated that the rate of the fast step of the porphyrin radical generation is independent of pH, whereas the slower step of ferryl-heme formation is dependent on pH. Simulation of the detailed pH dependence of the kinetics clearly shows that the deprotonation−protonation equilibrium of the protein matrix can control the ferryl-heme generation in a heme pocket of Mb.

Introduction

Chemical species with highly positive oxidation/reduction (redox) potentials play crucial roles in many biological reactions. In the biosynthesis of bioactive compounds or metabolism of toxic materials, for example, powerful oxidants are employed as key reactive species in the active sites of diverse enzymes such as monooxygenase, dioxygenase, peroxidase, and catalase.[1] Most systems include an inner sphere electron-transfer (ET) process from or to an active oxygen species. Another important example is the photosynthetic oxygen-evolving center (OEC) consisting of a Mn cluster in photosystem II.[2] After photoinduced ET from chlorophyll dimer P$_{680}$ to acceptors, the photooxidized P$_{680}$ (P$_{680}$$^+$) is reduced by the tetramanganase cluster of OEC. This step is apparently driven by the highly positive redox potential of P$_{680}$$^+$ (+1.12 V vs NHE). It has been speculated that a similar electron (or hole) transfer, driven by a highly positive redox potential, also occurs in ribonucleotide reductase.[3]

In the model studies for elucidation of biological ET, considerable efforts have been focused on ET processes driven by a highly negative redox potential. Most artificial model compounds were synthesized to mimic a primary charge separation event of photosynthesis or the downhill reactions of the respiration chain without investigating ET driven by highly positive redox potential.[4] Engineered proteins have been shown to be suitable model systems for determining ET events in natural proteins for the past decade.[5] However, there are

* To whom correspondence should be addressed. E-mail: itarutcm@mbox.nc.kyushu-u.ac.jp.

† Kyushu University.

‡ Institute of Molecular Science.

§ Kitasato University.

(1) (a) *Cytochrome P-450: Structure, Mechanism, and Biochemstry*; Ortiz de Montellano, P. R., Ed.; Plenum Press: New York, 1986. (b) Ortiz de Montellano, P. R. *Acc. Chem. Res.* **1987**, *20*, 289. (c) White, R. E.; Coon, M. J. *Annu. Rev. Biochem.* **1980**, *50*, 315. (d) *The Enzymes*; Sigman, D. S., Ed.; Academic Press: San Diego, 1992; Vol. 20. (e) *Peroxidases in Chemistry and Biology*; Everse, J., Everse, K. E., Grisham, M. B., Eds.; CRC Press: Boca Raton, FL, 1991; Vols. 1 and 2. (f) *Principles of Bioinorganic Chemistry*; Lippard, S. J., Berg, J. M., Eds.; USB Press: Mill Valley, CA, 1994.

(2) (a) Tommos, C.; Babcock, G. T. *Acc. Chem. Res.* **1998**, *31*, 18. (b) Hoganson, C. W.; Babcock, G. T. *Science* **1997**, *277*, 1953.

(3) (a) Reichard, P. *J. Biol. Chem.* **1993**, *268*, 8383. (b) Bollinger, J. J.; Edmondson, D. E.; Huynh, B. H.; Filley, J.; Norton, J. R.; Stubbe, J. *Science* **1991**, *253*, 292. (c) Stubbe, J. A. *Annu. Rev. Biochem.* **1989**, *58*, 257.

(4) For reviews, see: (a) Wasielewski, M. R. *Chem. Rev.* **1992**, *92*, 435. (b) Balzani, V.; Credi, A.; Venturi, M. *Curr. Opin. Chem. Biol.* **1997**, *1*, 506.

(5) (a) Marcus, R. A.; Sutin, N. *Biochim. Biophys. Acta* **1985**, *811*, 265. (b) Winkler, J. R.; Gray, H. B. *Chem. Rev.* **1992**, *92*, 369. (b) McLendon, G.; Hake, R. *Chem. Rev.* **1992**, *92*, 481. (c) Durham, B.; Millet, F. *J. Chem. Educ.* **1997**, *74*, 636. (d) Fenwick, C.; Marmor, S.; Govindaraju, K.; English, A. M.; Wishart, J. F.; Sun, J. *J. Am. Chem. Soc.* **1994**, *116*, 3169. (e) Fenwick, C. W.; English, A. M.; Wishart, J. F. *J. Am. Chem. Soc.* **1997**, *119*, 4758.

relatively few examples where highly *positive* redox potential, not *negative* redox potential, is the main driving force. Among the former type of study, a pioneer work was carried out using the flash quenching method developed by Gray, Winkler, and co-workers.[6] They recently succeeded in the intermolecular photooxidation of heme-model peptides (MP8) and horseradish peroxidase (HRP).[7] Unfortunately, however, the intermolecular electron-transfer process which is included in their systems made the reaction mechanism too ambiguous to be clearly understood. For the understanding of oxidative ET mechanisms, in general, it is necessary to construct an appropriate model in which the *intra*molecular ET is performed in the key steps of the reaction driven by a highly positive redox potential.[8] We have synthesized a semisynthetic myoglobin (Mb) bearing ruthenium tris-(2,2′-bipyridine) ($Ru(bpy)_3$-Mb) by cofactor reconstitution and consider it to provide a suitable model for intramolecular ET. Initially, we made an attempt to photoproduce the Ru^{3+} state by oxidative quenching and subsequently attempted to investigate the electron abstraction process of heme instead of electron injection using our engineered Mb.[9] In this paper, we describe our study on the phototriggered generation of oxidizing species in the Mb active site in detail. Importantly, the facilitated intramolecular ET makes it possible to detect directly a porphyrin cation radical as a key intermediate by laser flash photolysis. We have determined rate constants for the step of the generation of the porphyrin radical intermediate and for the subsequent ferryl-Mb generation step directly for the first time.

Results

Steady-State Photooxidation of $Ru(bpy)_3$-Mb. Chloropentamminecobalt(III) ($[Co(NH_3)_5Cl]^{2+}$) complex was employed as a sacrificial oxidative quencher for the photoexcited state of $Ru^{2+}(bpy)_3$.[10] Scheme 1 shows the order of the redox potentials of the chemical species related to this reaction. The redox potential of the ferryl-Mb (Fe^{4+}-heme) was found to be +0.896 V vs NHE.[11] Since $Ru^{3+}(bpy)_3$ is a powerful oxidant (+1.26 V vs NHE, comparable in value to P_{680}^+), the electron transfer from the resting state of met-Mb(Fe^{3+}) to $Ru^{3+}(bpy)_3$ was expected to be thermodynamically favorable.[12]

Scheme 1. Redox Potentials of the Chemical Species Related to the Reaction and Schematic Electron Abstraction of $Ru(bpy)_3$-Mb

Chart 1

1 (X= $-C_2H_4$-O-C_3H_6-)
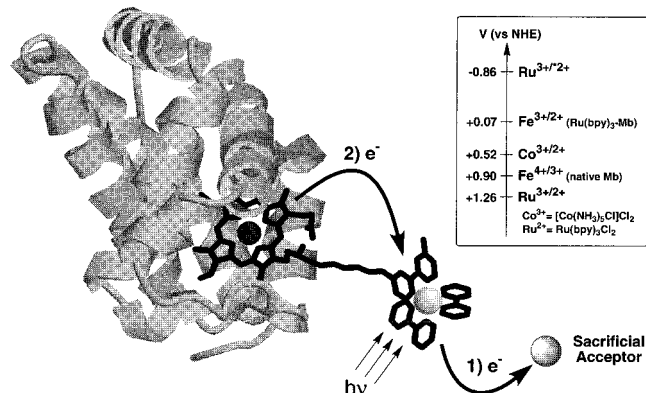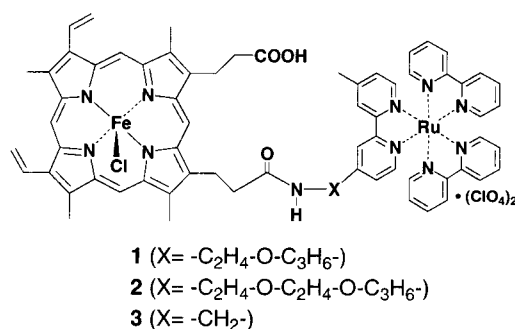2 (X= $-C_2H_4$-O-C_2H_4-O-C_3H_6-)
3 (X= $-CH_2$-)

$Ru(bpy)_3$-Mb **1** (Chart 1) was prepared by reconstitution of chemically modified heme **1** with apo-Mb according to our previously reported method.[13] To examine an effect of the spacer connecting $Ru(bpy)_3$ with heme, other heme derivatives (**2** or **3**) ($Ru(bpy)_3$-Mb **2** or **3**) were designed and synthesized. Hemes **2** and **3** were reconstituted according to the same method used for heme **1**. Visible light (>450 nm) irradiation to the deaerated aqueous solution containing $Ru(bpy)_3$-met-Mb (ferric (Fe^{3+}) state) in the presence of $[Co(NH_3)_5Cl]^{2+}$ caused a UV−vis spectral change as shown in Figure 1a. A strong peak at 408 nm and weak peaks at 505 and 630 nm due to the Soret- and Q-bands of ferric-Mb, respectively, decreased, and new peaks at 426, 540, and 560 nm increased. These changes were synchronous (inset of Figure 1a). The ferryl Mb was conventionally prepared by treatment of ferric-Mb with hydrogen peroxide (H_2O_2).[14] The difference spectra of the generated species in Figure 1a agree well with the difference spectra between H_2O_2-generated ferryl-Mb and ferric-Mb. The electron paramagnetic resonance (EPR) spectrum of $Ru(bpy)_3$-met-Mb before photolysis displayed a strong signal at $g = 6.0$ and a weak signal at $g = 2.0$, which are typical of the ferric high-spin state. These two peaks were weakened and almost disappeared after 65 min of photolysis (a very weak signal around $g = 2$, probably due to some organic radical, was observed).[15] When 2-methoxyphenol, a typical substrate of peroxidase enzymes, was added to the photooxidized $Ru(bpy)_3$-Mb, ferric-Mb was regenerated simultaneously with the disappearance of the photoproduced species as monitored by the UV−vis difference spectrum (Figure 1b). In addition, an extra

(6) (a) Chang, I.-J.; Gray, H. B.; Winkler, J. R. *J. Am. Chem. Soc.* **1991**, *113*, 7056. (b) Mines, G. A.; Bjerrum, M. J.; Hill, M. G.; Casmiro, D. R.; Chang, I.-J.; Winkler, J. R.; Gray, H. B. *J. Am. Chem. Soc.* **1996**, *118*, 1961.

(7) (a) Low, D. W.; Winkler, J. R.; Gray, H. B. *J. Am. Chem. Soc.* **1996**, *118*, 117. (b) Berglund, J.; Pascher, T.; Winkler, J. R.; Gray, H. B. *J. Am. Chem. Soc.* **1997**, *119*, 2464.

(8) (a) Hamachi, I.; Tanaka, S.; Shinkai, S. *Chem. Lett.* **1993**, 1417. (b) Hamachi, I.; Tanaka, S.; Shinkai, S. *J. Am. Chem. Soc.* **1993**, *115*, 10458. (c) Hamachi, I.; Tanaka, S.; Tsukiji, S.; Shinkai, S.; Oishi, S. *Inorg. Chem.* **1998**, *37*, 4380.

(9) Hamachi, I.; Tsukiji, S.; Tanaka, S.; Shinkai, S. *Chem. Lett.* **1996**, 751.

(10) (a) Gafney, H. D.; Adamson, A. W. *J. Am. Chem. Soc.* **1972**, *94*, 8238. (b) Navon, G.; Sutin, N. *Inorg. Chem.* **1974**, *13*, 2159. (c) Lehn, J.-M.; Sauvage, J.-P.; Ziessel, R. *Nouv. J. Chim.* **1979**, *3*, 423. (d) Shafirovich, V. Y.; Khannanov, N. K.; Strelets, V. V. *Nouv. J. Chim.* **1980**, *4*, 81.

(11) He, B.; Sinclair, R. Copeland, B. R.; Makino, R.; Powers, L. S.; Yamazaki, I. *Biochemistry* **1996**, *35*, 2413.

(12) Kalyanasundaram, K. *Coord. Chem. Rev.* **1982**, *46*, 159.

(13) (a) Hamachi, I.; Nakamura, K.; Fujita, A.; Kunitake, T. *J. Am. Chem. Soc.* **1993**, *115*, 4966. (b) Hamachi, I.; Tajiri, Y.; Murakami, Y.; Shinkai, S. *Chem. Lett.* **1994**, 575. (c) Hamachi, I.; Tajiri, Y. Shinkai, S. *J. Am. Chem. Soc.* **1994**, *116*, 7434. (d) Hamachi, I.; Nomoto, K.; Tanaka, S.; Shinkai, S. *Chem. Lett.* **1994**, 1139. (e) Hamachi, I.; Matsugi, T.; Tanaka, S.; Shinkai, S. *Bull. Chem. Soc. Jpn.* **1996**, *69*, 1657−1661. (f) Hamachi, I. Nagase, T.; Tajiri, Y.; Shinkai, S. *J. Chem. Soc., Chem. Commun.* **1996**, 2205. (g) Hamachi, I.; Tajiri, Y.; Nagase, T.; Shinkai, S. *Chem. Eur. J.* **1997**, *3*, 1025.

(14) (a) Yonetani, T.; Schleyer, H. *J. Biol. Chem.* **1967**, *242*, 1974. (b) King, N. K.; Winfield, M. E. *J. Biol. Chem.* **1963**, *238*, 1520.

(15) (a) Choe, Y. S.; Rao, S. I.; Ortiz de Montellano, P. R. *Arch. Biochem. Biophys.* **1994**, *314*, 126. (b) Wilks, A.; Ortiz de Montellano, P. R. *J. Biol. Chem.* **1992**, *267*, 8827.
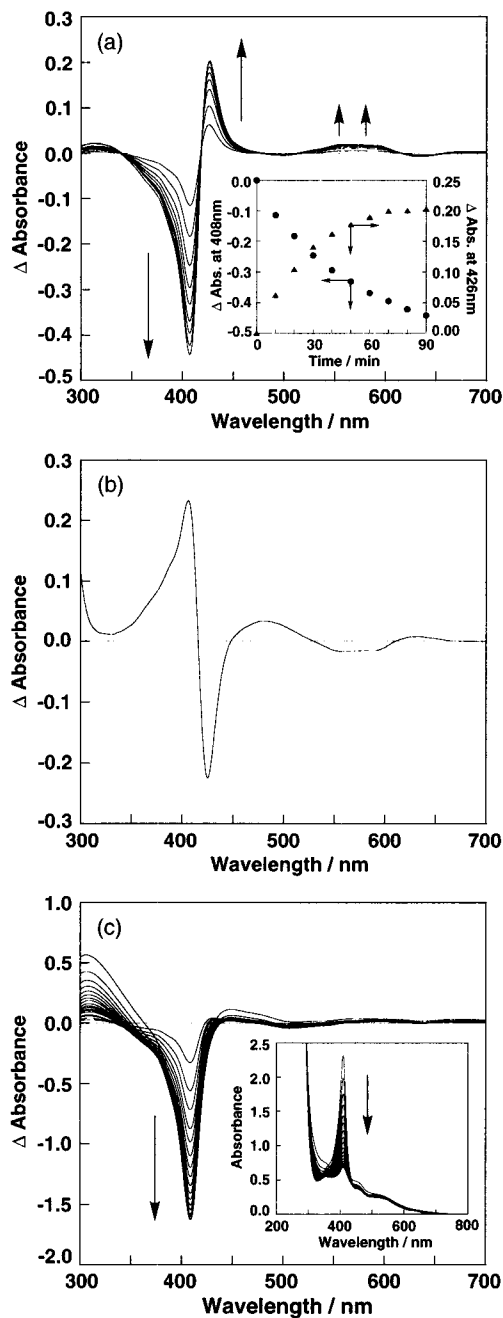
Figure 1. (a) Difference spectra of Ru(bpy)₃-Mb **1** upon steady-state photoirradiation. Conditions: [Ru(bpy)₃-Mb **1**] = 14 μM; [[Co(NH₃)₅-Cl]Cl₂] = 3 mM. Inset: Time courses of increase at 426 nm and decrease at 408 nm during photolysis. (b) Difference spectra of the photogenerated species of Ru(bpy)₃-Mb **1** upon the addition of 2-methoxyphenol. (c) Difference spectra of the intermolecular system upon steady-state photoirradiation. Conditions: [native Mb] = [Ru-(bpy)₃] = 14 μM; [[Co(NH₃)₅Cl]Cl₂] = 3 mM. Inset: The spectral change of this reaction. All experiments were performed in 50 mM phosphate buffer, pH 7.5, at 25 °C.

peak at 470 nm due to the one-electron oxidation product of 2-methoxyphenol slightly but definitely emerged.[16] These data are consistent with the photoproduction of the ferryl species in the buried active site of Mb. Circular dichroism (CD) spectroscopy, high-performance liquid chromatography (HPLC), and gel electrophoresis (SDS−polyacrylamide electrophoresis (PAGE)) of the resultant ferryl-Mb confirmed that photodamage of Mb did not occur upon ET.[17]

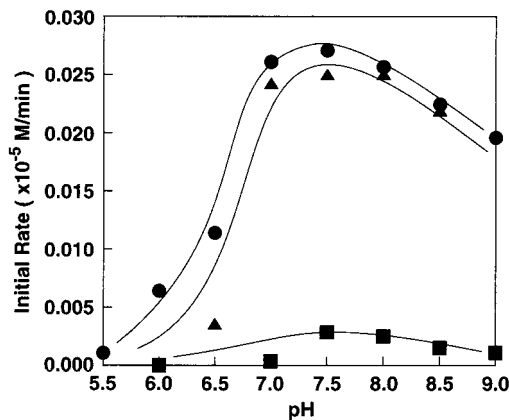(16) Maehly, A. C.; Chance, B. *Methods Biochem. Anal.* **1954**, *1*, 357.

Figure 2. pH dependence of the initial rates of photogeneration of ferryl-Mb. Conditions: [Ru(bpy)₃-Mb **1** (●), **2** (▲), **3** (■)] = 14 μM; [Co(NH₃)₅Cl]Cl₂] = 3 mM; pH 5.5−9.0. Initial rates were determined by dividing the slope obtained from the time trace of the absorbance (the inset of Figure 1a) by the difference molecular coefficient Δε between ferryl-Mb and ferric-Mb at 426 nm. All experiments were performed in either 50 mM phosphate or borate buffer at 25 °C.

Table 1. Quantum Yields of Photooxidation of Ru(bpy)₃-Mb **1**, **2**, and **3**[a]

	pH 6.0	pH 7.5	pH 9.0
Ru(bpy)₃-Mb **1** ($\times 10^{-4}$)	1.9 ± 0.3	10.3 ± 1.9	3.1 ± 0.1
Ru(bpy)₃-Mb **2** ($\times 10^{-4}$)	3.7 ± 0.2	8.2 ± 0.6	4.6 ± 0.7
Ru(bpy)₃-Mb **3** ($\times 10^{-4}$)	0	1.0 ± 0.4	0.3 ± 0.2
intermolecular system	0	0	0

[a] At 25 °C under Ar atmosphere, [[Co(NH₃)₅Cl]Cl₂] = 3 mM, 50 mM KH₂PO₄ buffer.

Next, we conducted a control experiment using an intermolecular reaction system (an equimolar mixture of Ru(bpy)₃ and native Mb in the presence of [Co(NH₃)₅Cl]²⁺). As shown in Figure 1c, new peaks due to ferryl-Mb did not appear during photolysis and peaks due to ferric-Mb were greatly reduced to become a noncharacteristic broad spectrum.[18] It is evident that the photoinduced reaction of the intermolecular control system is different from the intramolecular reaction of the Ru(bpy)₃-Mb system.

Figure 2 shows the pH dependence of the initial rate of the photogeneration of ferryl-Mb. At acidic pH (below pH 6), no reaction occurred. The initial rate was greatly accelerated at neutral pH (pH 6.5−7.5) and slightly declined at basic pH (pH 8.0−9.0). Ru(bpy)₃-Mb **2**, having a longer spacer, showed behavior similar to that of the above-mentioned Ru(bpy)₃-Mb **1** in both the initial rate values and its pH dependence. The photooxidation efficiency for Ru(bpy)₃-Mb **3** having a short spacer was very low over the wide pH range (pH 5.5−9.0), compared to the other Ru(bpy)₃-Mbs. The quantum yields (Φ) of these derivatives are summarized in Table 1. The order is in good agreement with that of the initial rate data shown in Figure 2.[19]

Laser Flash Photolysis Study. To investigate the reaction kinetics in detail, laser flash photolysis experiments were conducted. The excited *Ru²⁺(bpy)₃ was oxidatively quenched

(17) In contrast, for the intermolecular reaction, negative peaks at 208 and 222 nm and a positive peak at 195 nm due to a typical α-helix in the CD spectrum are gradually lessened and lost during photolysis. The results obtained from HPLC showed that, during the photolysis, the peak intensity due to protoheme and the protein skeleton is reduced for the intermolecular system. In SDS−PAGE, the original band due to apo-Mb is smeared, and several bands are observed. These suggest that the Mb structure was considerably damaged in the intermolecular photooxidation process.

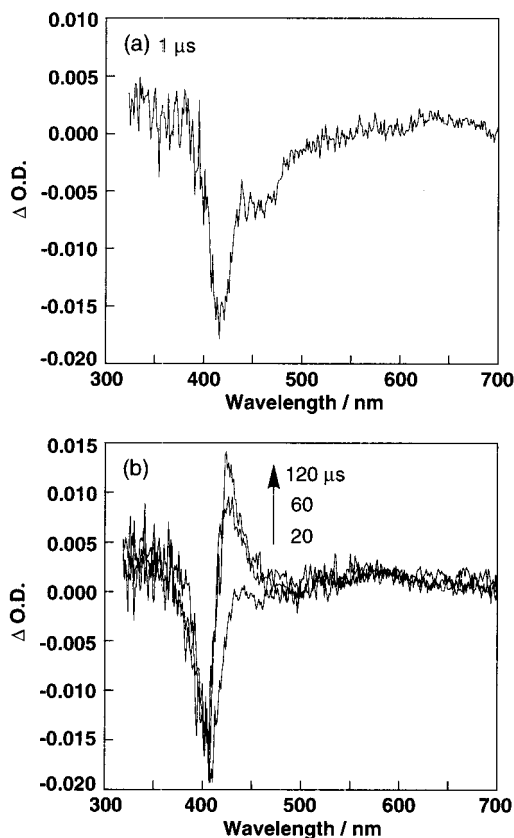(18) A sharp Soret-band is never regenerated by addition of 2-methoxyphenol.

Phototriggered Oxidation of Ferric- to Ferryl-Heme

J. Am. Chem. Soc., Vol. 121, No. 23, 1999 5503

Figure 3. Transient absorption spectra monitored at (a) 1 μs and (b) 20−120 μs after laser flash photolysis of Ru(bpy)$_3$-Mb **1**. Conditions: [Ru(bpy)$_3$-Mb **1**] = 20 μM; [[Co(NH$_3$)$_5$Cl]Cl$_2$] = 3 mM; 50mM phosphate buffer; pH 7.5; 20 °C.
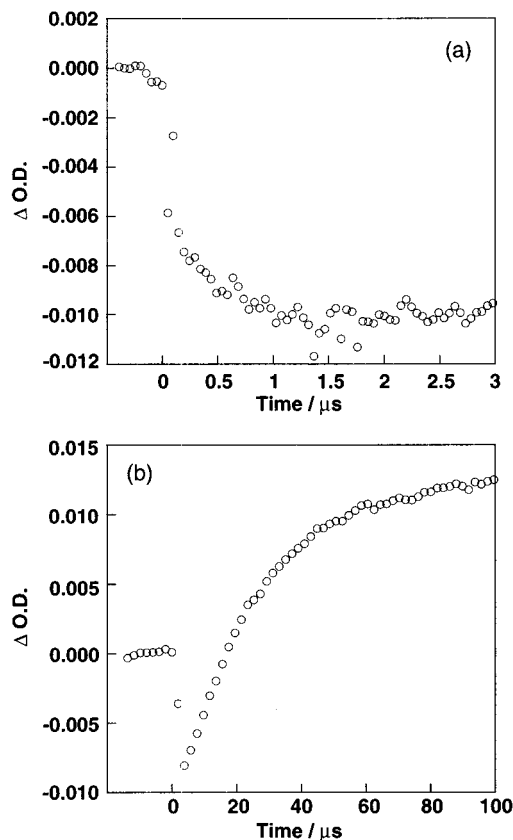

Figure 4. Typical kinetic trace for Ru(bpy)$_3$-Mb **1**: (a) at 426 nm in a 3 μs time range, (b) at 426 nm in a 100 μs time range. Data points from 0 to 1 μs in (a) and from 0 to 40 μs in (b) were used for fitting. These correlation coefficients for each analysis were satisfactory (0.940 and 0.998 for k_1 and k_2, respectively). Conditions: [Ru(bpy)$_3$-Mb **1**] = 20 μM; [[Co(NH$_3$)$_5$Cl]Cl$_2$] = 3 mM; 50 mM phosphate buffer; pH 7.5; 20 °C.

by a Co(III) complex within 0.04 μs. Transient absorption of the intramolecular Ru(bpy)$_3$-Mb **1** is shown in Figure 3. At 1 μs following laser pulses, a simple bleaching of a Soret band region was detected (Figure 3a). Then, in the time range of 20− 120 μs, a new peak at 426 nm rose and intensified (Figure 3b). This spectral change suggests that the kinetics are biphasic. The first step is a fast reaction, reaching completion within 5 μs after laser photolysis. This stage is monoexponential, and the first-order rate constant (k_1) was determined to be 7.1 × 10^5 s^{-1} by tracing the absorption change at 426 nm (Figure 4a). The difference spectrum in this fast reaction is in close accord with that of an electrochemically generated iron(III)-tetraphe-nylporphyrin cation radical or the protoporphyrin cation radical of photooxidized microperoxidase (MP8) (under acidic conditions), suggesting that the fast bleaching of the Soret-band is attributable to the oxidation of the porphyrin ring.[7a,20] In contrast, the difference spectra of the much slower second step, following the fast process, agree well with the difference spectra between ferryl-Mb and ferric-Mb obtained in the steady-state photolysis as shown in Figure 1a, indicating that the slow process can be ascribed to the formation of the ferryl-heme of Mb. The time course of absorbance at 426 nm (Figure 4b) in the slower process (10−100 μs range) also gave a single-exponential curve with a first-order rate constant (k_2) of 4.0 × 10^4 s^{-1}. Figure 5 displays

the pH dependence of the reaction rates of these two steps in Ru(bpy)$_3$-Mb **1**. The rate of the first step is practically independent of pH within the experimental errors (Figure 5a), which is reasonably explained by the proton uncoupling of the porphyrin ring oxidation.[21] On the other hand, the reaction of the second step is gradually accelerated with an increase of the pH value (Figure 5b). This step can be considered as a proton-coupling process. When the flash photolysis experiments are conducted in D$_2$O solution, we can compare the isotope effects in each step. It is clear that the k_1 values in H$_2$O are identical with those in D$_2$O (k_1(H)/k_1(D) = 1.1−1.0), whereas the k_2 values in H$_2$O are greater than those in D$_2$O (k_2(H)/k_2(D) = 1.8 at pH 6.0, 2.5 at pH 7.5, and 4.6 at pH 9.0).

The rate of the first step for Ru(bpy)$_3$-Mb **2** (k_1 = 2.0 × 10^5 s^{-1}) is slightly slower than that for Ru(bpy)$_3$-Mb **1**, but the second step proceeds with an identical rate (k_2 = 4.0 × 10^4 s^{-1} at pH 7.5). These observations are not inconsistent with the above-proposed mechanism. In the case of the shortest spacer (Ru(bpy)$_3$-Mb **3**), the emission lifetime of the excited Ru(bpy)$_3$ was too short to be measured by our instruments (5 ns laser pulse width) and we did not detect any transient absorption after laser excitation in the presence of Co(III). For the transient absorption of the intermolecular control, the bleaching of Ru-(bpy)$_3$ at 450 nm due to the photooxidation by Co(III) complex and the slow recovery were detected simply.

(19) We have previously determined that the ET rate from photoexcited Ru^{2+}(bpy)$_3$ to the ferric center of Mb is 4.4 × 10^7 or 3.7 × 10^7 s^{-1} for Ru(bpy)$_3$-Mb **1** or Ru(bpy)$_3$-Mb **2**, respectively. The kinetics of Ru(bpy)$_3$-Mb **3** could not be estimated due to the short lifetime of the charge separated state. The order of the efficiency for the photoreduction of Ru(bpy)$_3$-Mbs was also the same as that of the present case (i.e., Ru(bpy)$_3$-Mb **1** = Ru-(bpy)$_3$-Mb **2** ≫ Ru(bpy)$_3$-Mb **3**).[8c]

(20) Gans, P.; Buisson, G.; Duée, E.; Marchon, J.-C.; Erler, B. S.; Scholz, W. F.; Reed, C. A. *J. Am. Chem. Soc.* **1986**, *108*, 1223.

(21) At pH 9.0, the second step is accelerated too fast for one to separately determine the k_1 values. In D$_2$O, however, the second step is still slow enough to estimate the k_1 at pH 9.0 independently.

Discussion

Using the intramolecular electron abstraction reaction by $Ru^{3+}(bpy)_3$, an oxidative ferryl species was photoproduced in the active site of the semisynthetic $Ru(bpy)_3$-Mbs. The photo-oxidation mechanism was roughly described as follows:
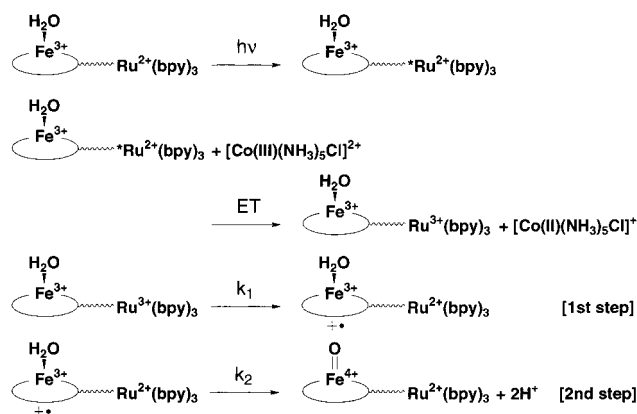
At the initial stage, the photoexcited $Ru^{2+}(bpy)_3$ is oxidatively quenched by $[Co(NH_3)_5Cl]^{2+}$, a sacrificial acceptor, to give $Ru^{3+}(bpy)_3$. $Ru^{3+}(bpy)_3$ thus formed efficiently abstracts an electron from the porphyrin ring (the first step with a first-order rate constant k_1 of 7.1×10^5 s^{-1}),[22] followed by the iron oxidation (the second step) by the porphyrin radical. The photogeneration of the ferryl-Mb was not observed in the intermolecular system by either steady-state photolysis or laser flash photolysis.

Significantly, the laser photolysis experiments of $Ru(bpy)_3$-Mbs demonstrated that the photogeneration of ferryl-Mb proceeds via the porphyrin cation radical. The porphyrin cation radical, proposed as an intermediate in MP8 photooxidation, can be detected for the first time using an accelerated *intra*molecular electron transfer as a key step.[23] In the previous study of MP8 by Gray's group, the electron abstraction step was rather slow, relative to the following iron oxidation step. In the HRP case, a slower water coordination step before the ferryl species formation prevented the quantitative determination of the kinetic value for the ferryl-heme generation step. The direct detection of a key intermediate not only confirmed the photooxidation mechanism of hemoproteins proposed by Gray, Winkler, and co-workers[7] but also made it possible to determine the rate constants for each step of the photooxidation of $Ru(bpy)_3$-Mbs.

Detailed pH dependence studies clearly propose an overall scheme for the photooxidation of $Ru(bpy)_3$-Mbs.[24] The rate of

(22) The lifetime of $Ru^{3+}(bpy)_3$ in $Ru(bpy)_3$-Mb was determined to be 2 μs by monitoring the recovery of the bleached $Ru^{2+}(bpy)_3$, which is in good agreement with $1/k_1$.

(23) Although the intramolecular rate constant (k_1) cannot be directly compared to the intermolecular rate constants for MP8 and HRP, k_1 was still more than 10^3-fold greater than the pseudo-first-order rate constant for HRP (300 s^{-1}), in which the heme is buried in the protein matrix, like that of Mb.[7b] It is also 20 times greater than the corresponding pseudo-first-order rate for MP8 bearing the heme exposed to the solvent.[7a] These suggest the advantage of *intra*molecular electron abstraction by Ru^{3+}-$(bpy)_3$.

(24) The dependence of the steady-state photooxidation rate on pH was found to be rather inconsistent with that of k_2 under the higher pH region. It is known that the decomposition of the Co(III) ammine complex upon oxidation requires five protons as shown in the following reaction: $[Co^{III}(NH_3)_5Cl]^{2+} + e^- + 5H^+ + 6H_2O \rightarrow [Co^{II}(H_2O)_6]^{2+} + 5NH_4^+ + Cl^-$. Thus, deceleration of the steady-state rate in the basic pH region can be explained by lessening the sacrificial acceptability of the Co(III) ammine complex under basic pH.[10]
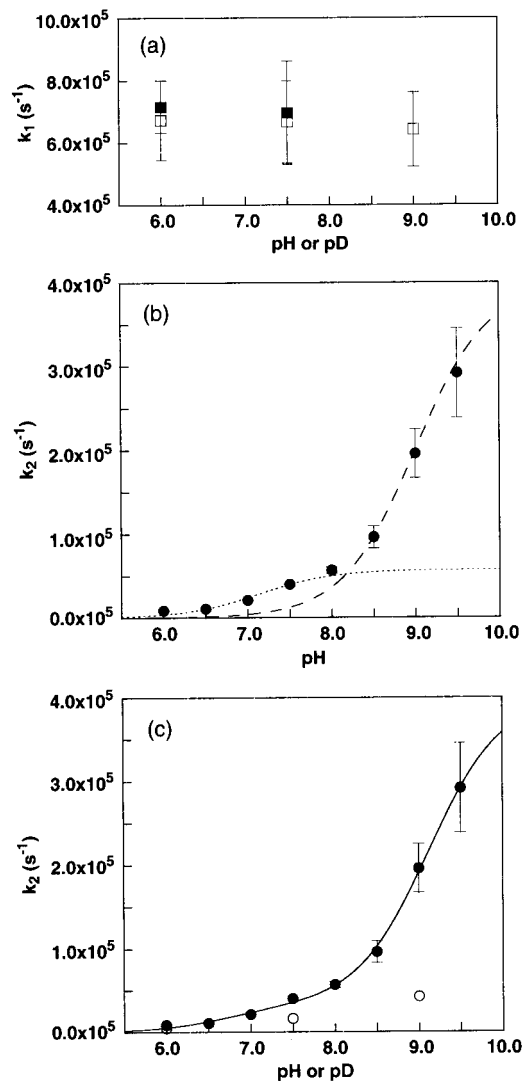
Figure 5. pH dependence of the photooxidation process of $Ru(bpy)_3$-Mb **1**: (a) Dependence of the rate of the porphyrin radical formation step (k_1) on pH or pD; closed squares (■) for k_1 in H_2O and open squares (□) for k_1 in D_2O. (b) Dependence of the rate of the ferryl-Mb formation step from the porphyrin radical (k_2). Fitting curves followed by eq 4 or eq 8 in the text are given by the dotted line or the broken line, respectively. (c) Curve fitting of the experimental data in the entire pH range of H_2O followed by eq 9 in the text is given by the solid line; closed circles (●) for k_2 in H_2O and open circles (○) for k_2 in D_2O. Data points are the average of 3–5 kinetic runs. The errors in the data points are in the range of 1–24% of the average. The error bars that do not appear are smaller than the data points. Conditions: $[Ru(bpy)_3$-Mb **1**$] = 20$ μM; $[[Co(NH_3)_5Cl]Cl_2] = 3$ mM; 20 °C; pH was adjusted using either 50 mM phosphate buffer (pH 6.0–8.0) or 50 mM borate buffer (pH 8.5–9.5).

the ferryl-Mb formation step (k_2) including proton/electron-transfer processes is accelerated with the increase of pH, unlike the pH independence of k_1. Furthermore, we observed the isotope effect in the second step (k_2), but not in the first step (k_1). Since the pK_{a0} value of the coordinated water of $Ru(bpy)_3$-met-Mb **1** was spectrophotometrically determined to be 7.9, met-Mb **1** mainly exists in an Fe(III)-H_2O form at acidic pH (pH below 7.5) and in an Fe(III)-OH form at basic pH (pH above 8.5) as a resting state.[8c] To analyze the reaction scheme simply, we initially considered the reaction under acidic pH conditions where the initial state is predominant in an Fe(III)-H_2O form. The above-mentioned equilibrium isotope effect suggests that a deprotonated form of Mb is the active species in the ferryl-
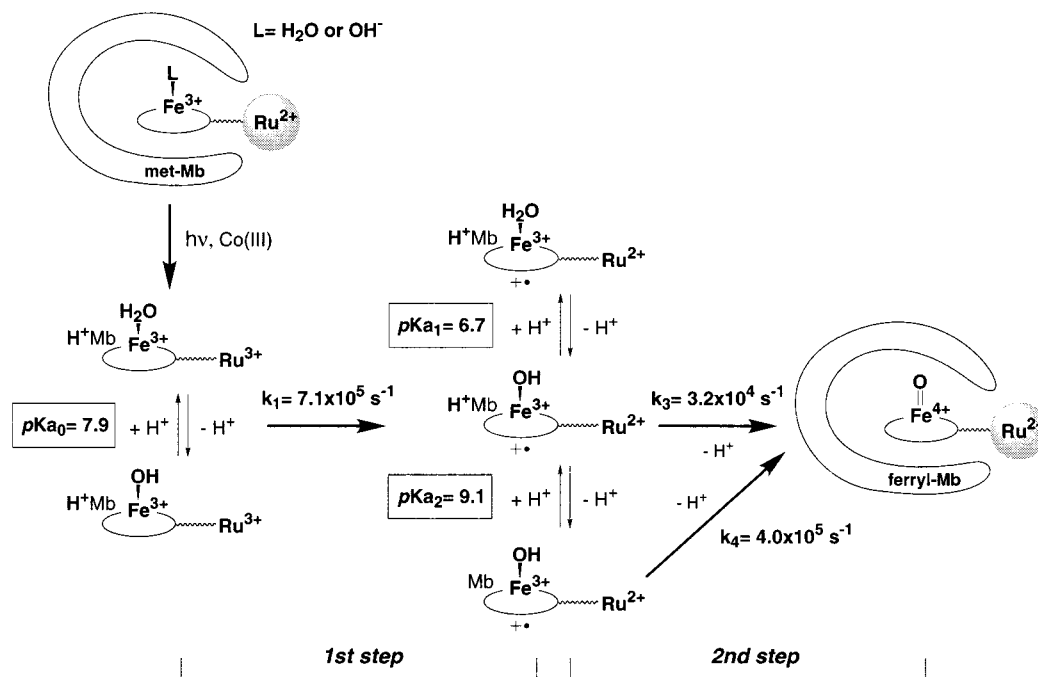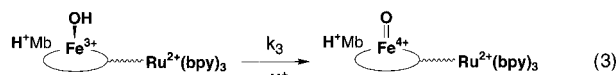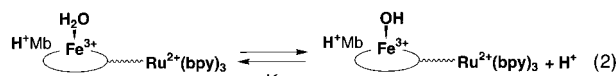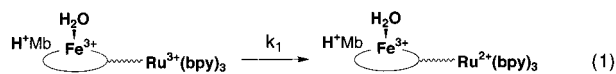
Figure 6. Overall scheme of the phototriggered electron abstraction reaction using Ru(bpy)$_3$-Mbs.

Mb generation step as follows:[25]

$$k_2'(\text{app}) = \frac{k_3}{K_1[\text{H}^+] + 1} \quad (4)$$

Since K_1 is defined as a protonation constant here, the corresponding pK_{a1} value can be calculated from log K_1. From the curve-fitting analysis at the acidic conditions, we preliminarily obtained pK_{a1} and k_3 values of 7.1 and 5.7 × 10^4 s^{-1}, respectively. But unfortunately, the simulation curve did not fit the experimental data under basic pH (see the dotted line of Figure 5b). Above the pK_{a0}, on the other hand, an Fe(III)-OH species exists predominantly in the resting form. In this case, eq 2 is negligible due to the low pK_a and, instead, another equilibrium (eq 6) should be involved. Thus, the following mechanism is suggested at basic pH:[25]
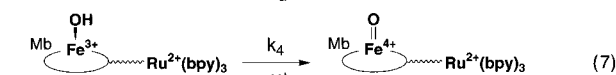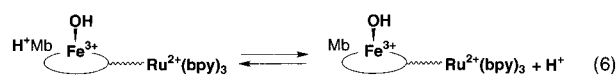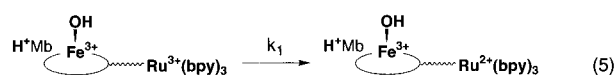
Since K_2 is defined as a protonation constant, the corresponding pK_{a2} value can be calculated from log K_2. Fitting the k_2'(app) values to eq 8 on the basic side yielded pK_{a2} and k_4 values of

$$k_2'(\text{app}) = \frac{k_4}{K_2[\text{H}^+] + 1} \quad (8)$$

9.0 and 4.0 × 10^5 s^{-1}, respectively. This curve, however, did not show good agreement with the experimental data points under acidic pH (the dashed line of Figure 5b). Finally, the combined reaction routes in the whole pH range can give the overall photooxidation scheme as shown in Figure 6. The relationship of k_2(app) with [H$^+$] can be redescribed as eq 9.

$$k_2(\text{app}) =$$
$$\frac{k_3(K_1 K_2[\text{H}^+]^2 + K_2[\text{H}^+] + 1) + k_4(K_1[\text{H}^+] + 1) - k_3}{(K_1[\text{H}^+] + 1)(K_1 K_2[\text{H}^+]^2 + K_2[\text{H}^+] + 1)} \quad (9)$$

Using the preliminary calculated data of pK_{a1}, pK_{a2}, k_3, and k_4 as initial values, the curve fitting from data over the entire pH range (pH 6.0−9.5) yielded precisely the corresponding values: pK_{a1}, pK_{a2}, k_3, and k_4 of 6.7, 9.1, 3.2 × 10^4 s^{-1}, and 4.0 × 10^5 s^{-1}. Figure 5 displays that the experimental data completely fit the simulation curve in the entire pH range.[26] Interestingly, the pK_a of the coordinated water shifted to the acidic region by 1.2 pH units as a result of formation of the cation radical. This is ascribed reasonably to a favoring of a hydroxide form in the electron-deficient porphyrin cation radical, rather than an aqua form. The pK_{a2} value is too acidic to be regarded as a simple pK_a of Fe(III)-OH. In addition, the generation of an Fe(III)-O$^-$ anion species is not plausible because the heme pocket of Mb is very hydrophobic. Instead, this may be attributed to an acid−base equilibrium of some residues in the Mb matrix. Although the residue has not been

The above mechanism affords a simple relationship between the apparent k_2 (k_2'(app)) and proton concentration [H$^+$]:

(25) In eqs 3 and 7, it is not clear so far that electron and proton transfers are concerted or stepwise. It is only insisted that this process includes one kinetic rate needed for fitting the present pH dependence.

(26) Since we have only three data points in D$_2$O, we cannot conduct the curve-fitting analysis.

identified yet, Lys 45 is one of the most promising candidates.[27] The distal His 64 can directly interact with ligands of Mb, but the pK_a is reported to be much lower (3.8 or 6.0, at the closed or the open conformation of the heme pocket, respectively).[28] It has been reported that the pK_a and the orientation of the imidazole ring of His 64 is influenced by Lys 45 (in horse or pig Mb) or Arg 45 (in sperm whale Mb).[29] It is possible, therefore, to consider that the protonation/deprotonation state of ϵ-N of Lys 45 indirectly regulates the orientation of His 64, so as to facilitate deprotonation of the hydroxide ligand in the heme pocket.[30] The most important finding in the detailed kinetics is that k_4 is 10-fold greater than k_3, indicating that deprotonation accelerates the formation of ferryl-Mb. Conceivably, the protein matrix controls the generation of a high-valent iron species through the conformational changes triggered by the protonation−deprotonation equilibrium.

In conclusion, this study shows that a phototriggered intramolecular electron abstraction is useful for trapping a short-lived active intermediate in an oxidation reaction in a protein matrix. We now intend to detect and estimate the decay of compound I of Mb (ferryl-heme/porphyrin radical), which has never been observed in the native Mb matrix, as the extension of this technique.[31]

Experimental Section

Materials. Horse heart myoglobin was purchased from Sigma. The synthesis of protohemins tethered to Ru(bpy)$_3$ has been reported previously.[8c] Pentaamminechlorocobalt(III) chloride ([Co^{III}(NH$_3$)$_5$Cl]-Cl$_2$) was synthesized according to a literature method.[32] Other chemicals were used as received.

Reconstitution of Ru(bpy)$_3$-Hemins 1, 2, and 3 with apo-Mb. Preparation of apo-Mb and reconstitution with the Ru(bpy)$_3$-Hemin has been reported previously.[8b,8c] Ferryl-Mb **1**, **2**, or **3** was formed by the addition of excess H$_2$O$_2$ (5-fold), and the molar absorption coefficient of ferryl-Mb was determined to be 7.4 × 10^4 (Ru(bpy)$_3$-Mb **1**), 6.0 × 10^4 (Ru(bpy)$_3$-Mb **2**), and 10.5 × 10^4 (Ru(bpy)$_3$-Mb **3**) M^{-1} cm^{-1}.

Steady-State Photolysis Experiments. The concentration of Ru-(bpy)$_3$-Mb **1**, **2**, or **3** solution was determined from the absorption at the Soret-band. [Co^{III}(NH$_3$)$_5$Cl]Cl$_2$ was added to Ru(bpy)$_3$-Mb dissolved in 50 mM phosphate or borate buffer. After the pH was adjusted with aqueous NaOH to the desired value, the solutions were degassed by freeze−pump−thaw cycles. Photoirradiation to the solutions was carried out using a 400 W high-pressure Hg lamp equipped with an optical filter ($\lambda > 450$ nm, Toshiba Y-45 glass filter) at 25 °C. Absorption

spectral changes were monitored by an UV−vis spectrophotometer (Shimadzu UV-160 or Hitachi U-3300).

Quantum Yields of the Photogeneration of Ferryl-Mb. Quantum yields of the photoactivation for Ru(bpy)$_3$-Mb **1**, **2**, and **3** were determined according to a slight modification of a literature procedure.[33] A 400 W Xe lamp (Ushio) equipped with a cutoff optical filter below 450 nm and a CuSO$_4$ solution was used. The light intensity absorbed by the solutions was measured by the use of potassium ferrioxalate (150 mM) as an actinometer.

Laser Photolysis Experiments. Sample solutions similar to those of steady-state photolysis (3 mL, quartz cell) degassed with five cycles of freeze−pump−thaw treatment were subjected to pulsed-laser photolysis at 20 °C, using third harmonic light (355 nm, fwhm = 5 ns) from a Q-switched Nd:YAG laser (Quanta-Ray DCR-11) for excitation. A right-angle optical system was employed for the excitation-analysis setup. Probe lights were detected by a photomultiplier tube (Hamaphoto R446) or a photodiode array (Princeton IRY-1024G/RB, gate width 4 ns).

Miscellaneous. EPR measurements were done with a JEOL JES-2X X-band spectrometer at liquid helium temperature. CD spectra were measured with a Jasco J-720 spectropolarimeter at 25 °C (signals were averaged at least 10 times, and the solvent baseline was subtracted). HPLC was carried out on a system consisting of a HITACHI L-7100 pump and a L-7400 detector (monitored at 220 nm) coupled to a D-7500 integrator (on a YMC−Pack ODS-A column (4.6 × 250 mm) and eluted with a linear gradient from H$_2$O to acetonitrile (containing 0.1% trifluoroacetic acid)). SDS−PAGE was performed according to the procedure reported by Laemmli[34] with a BIO-RAD Mini-PROTEAN II system. The nonlinear least-squares curve-fitting analyses were carried out by using KaleidaGraph Software (SYNERGY SOFTWARE). For the curve-fitting analyses shown in Figure 5b, four data points under the acidic region and three data points under the basic region, all of which include at least three experimantal data, were used. All points with no weighting factor were used for the fitting analysis under the entire pH range in Figure 5c. The correlation coefficient is estimated to be 0.999.

Supporting Information Available: Table listing the rate constants k_1 and k_2 (PDF). This material is available free of charge via the Internet at http://pubs.acs.org.

JA984199F

(27) To our knowledge, the pK_a of ϵ-N of Lys 45 of Mb has not been determined yet. However, the pK_a of ϵ-N of Lys in general is about 10 ± 1. See: *Biochemistry,* 3rd ed.; Stryer, L., Ed.; Freeman: New York, 1988.

(28) Morikis, D.; Champion, P. M.; Springer, B. A.; Sligar, S. G. *Biochemistry* **1989**, *28*, 4791.

(29) Carver, P. E.; Olson, J. S.; Smerdon, S. J.; Krzywda, S.; Wilkinson, A. J.; Gibson, Q. H.; Blackmore, R. S.; Ropp, J. D.; Sligar, S. G. *Biochemistry* **1991**, *30*, 4697.

(30) To specify the residue having a pK_a of 9.1 in Ru(bpy)$_3$-Mb, more physicochemical experiments using various mutant Mbs are required.

(31) Matsui, T.; Ozaki, S.; Watanabe, Y. *J. Biol. Chem.* **1997**, *272*, 32735.

(32) Schlessinger, G. G. *Inorg. Synth.* **1967**, *9*, 160.

(33) Hatchard, C. G.; Parker, C. A. *Proc. R. Soc. London, Ser. A* **1956**, *235*, 518.

(34) Laemmli, U. K. *Nature* **1970**, *227*, 680.